

The LHCb L0 trigger and related detectors

A. Satta, on behalf of the LHCb Collaboration

Università La Sapienza and INFN di Roma, e-mail: alessia.satta@roma1.infn.it

Received: 19 August 2003 / Accepted: 26 February 2004 /
Published Online: 13 July 2004 – © Springer-Verlag / Società Italiana di Fisica 2004

Abstract. The LHCb experiment will study CP violation and other rare phenomena using the b-hadrons produced at the LHC. A powerful trigger system is mandatory to select efficiently the b-hadron decays of interest out of the 40 MHz input rate keeping the output rate to an acceptable level for tape storage. The trigger system is divided in three levels. In this document an overview of the first trigger level, L0, and the related detectors is given.

PACS. 2 5.70.Ef – 21.60.Gx – 27.30.+t

1 Introduction

The LHCb experiment, now in preparation at CERN, will study the CP violation and rare decays in the b-hadron sector exploiting the large number of $b\bar{b}$ pairs generated at the Large Hadron Collider (LHC). The b and \bar{b} -hadrons produced in high energy pp collisions, $\sqrt{s} = 14$ TeV, are predominantly produced in the same forward or backward cone. It leads to a fixed-target like structure of the experimental setup which is depicted in Fig. 1. For details see [1].

At the LHC energy the non-elastic cross-section is predicted to be very high, around 80 mb [2]. To reduce detector radiation damage and to simplify the events reconstruction, the experiment plans to work at an average luminosity of $2 \cdot 10^{32} \text{cm}^{-2} \text{s}^{-1}$, two orders of magnitude lower than the maximum machine design value. At such luminosity the rate of crossings with interactions inside the detector acceptance is expected to be about 10 MHz, while the machine bunch crossing rate is 40 MHz. The trigger has to reduce this high rate down to 200 Hz before the data will be written to permanent storage. The rate of interesting events is much lower than the interaction rate, in fact the $b\bar{b}$ production cross section is 2 orders of magnitude less than the total cross section, and many of the interesting decay channels have very small visible branching ratios, even as low as 10^{-7} . The trigger that efficiently selects those rare events while reducing the input rate by five orders of magnitude is very challenging.

To select the interesting events the trigger will exploit the two typical signatures of the b-hadron: its large mass and its finite lifetime. The selection is performed in three stages:

- the level-0 trigger will reduce the input rate using calorimeters, the muon system and a dedicated part of the VELO detector (Pile-Up) down to a level at which all detector data can be digitized. L0 will mainly select

events containing high transverse momentum leptons, hadrons or photons.

- The level-1 trigger will reduce the 1 MHz L0 output rate to 40 kHz using the VELO and TT detectors and the high P_T candidates already found at L0. It will select events containing tracks with large impact parameter and large P_T .
- The high level trigger will reduce to 200 Hz the output rate using all detector information but RICHes. It will select interesting events confirming the L1 decision with better resolution or applying specific final state selection cuts.

The first trigger level is the subject of this document: in the next section the L0 strategy is summarized, while in the next three following sections the calorimeters, muon system and the Pile-Up Veto detectors are briefly described and their usage in the L0 trigger is explained. Section 6 describes how the L0 Decision Unit combines the information of all sub-triggers what performance is obtained.

2 L0 design

L0 exploits the b-hadrons signature of having high transverse momentum tracks as decay products. In particular it will search for high E_T electrons, hadrons or photons candidates using the calorimeter energy deposit information, while the muon stations are used for high P_T muon search.

Using global variables, like the multiplicity of deposits in the calorimeter, or the number of pp interactions in a crossing, it will also reject crowded events. Otherwise such events will occupy disproportional bandwidth at L0 and will increase the latency of the higher trigger levels. Moreover the rejection of background and a correct tagging is much more difficult in those high multiplicity events.

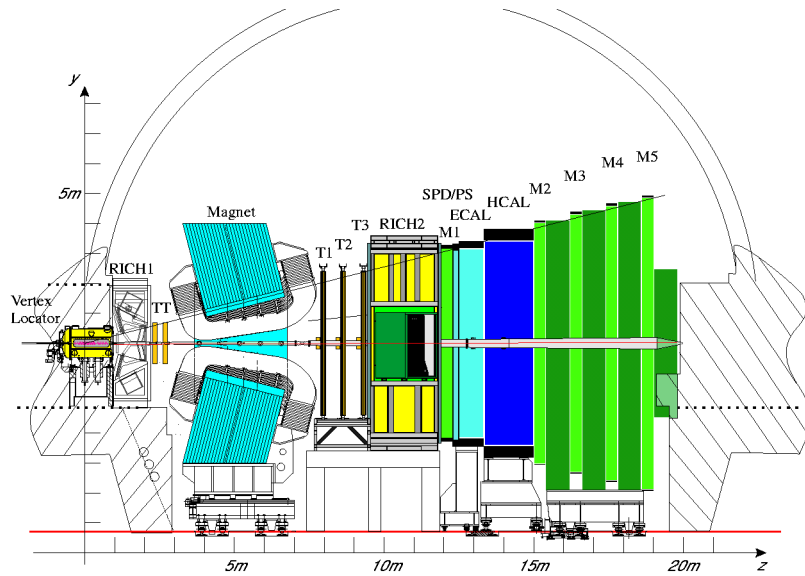


Fig. 1. A side view of the LHCb detector. The vertex detector (VELO), four tracking stations (TT, T1-T3), two RICHes for particle identification, the magnet, the electromagnetic (ECAL) and hadronic (HCAL) calorimeters and five muon stations (M1-M5) are shown

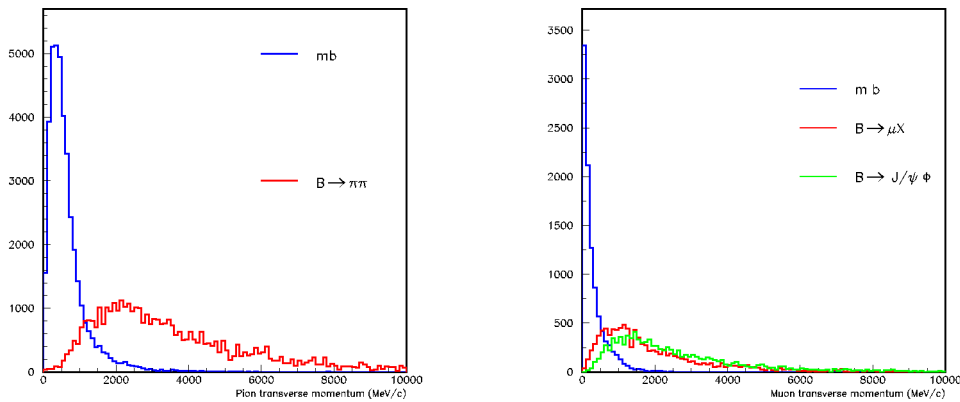


Fig. 2. On the *left* the E_T distribution for hadrons in minimum bias and in $B \rightarrow \pi\pi$ events. On the *right* the muon P_T distribution for minimum bias, $B \rightarrow \mu X$ and $B \rightarrow J\psi(\mu\mu)\phi$ events

Global variables cuts should reduce the input rate to about 9 MHz, thus the high transverse energy selection needs to get a reduction factor of nine. Such a moderate factor allows to use a “medium” cut on P_T : e.g about 3.5 GeV for hadrons, 2.5 GeV for photons and 1.2 GeV for muons (see Fig. 2).

The hardware implementation of all L0 trigger subsystems is fully pipelined and synchronous and uses non-custom components. The whole system, apart from some calorimeter trigger boards, is located behind the shielding wall in a radiation-free environment. The latency of the L0 trigger is fixed to 4 μ s including the time of flight and cable lengths. The time reserved for the L0 algorithms is about 1 μ s.

3 Calorimeter: The detector and its use in L0

The calorimeter detector is composed of four parts: the SPD (Scintillating Pad Detector), the preshower, the electromagnetic and the hadronic calorimeters. A schematic view of the calorimeter is depicted in Fig. 3 (for details see [3]).

The SPD and the preshower are two scintillating planes of 15mm thickness interspaced with a 12 mm ($2.5 X_0$) thick lead wall. The SPD is used to identify charged particles, allowing to distinguish between electrons and photons, while the preshower is used to identify the electromagnetic particles. The shashlik technology has been chosen for the electromagnetic calorimeter. The sampling structure of 2 mm lead sheets interspaced with 4 mm thick scintillating plates results in an energy

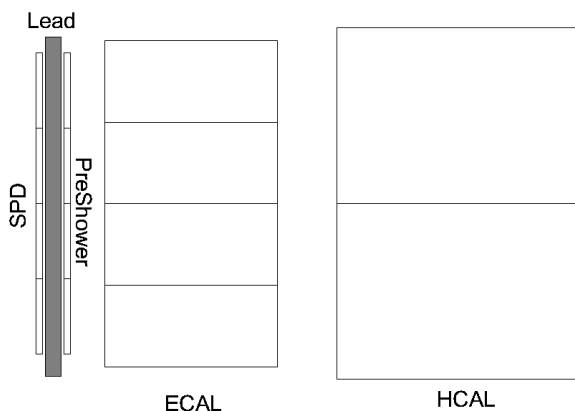


Fig. 3. Schematic view of the calorimeter system

resolution of $\sigma(E)/E = 10\%/\sqrt{E} \oplus 1.5\%$ (E in GeV). The total depth is 835 mm corresponding to $25 X_0$ and $1.1 \lambda_I$.

The hadronic calorimeter has a structure of iron/scintillating tiles, placed parallel to the beam. The total depth is 1655 mm corresponding to $5.6 \lambda_I$. The energy resolution for hadronic showers is $\sigma(E)/E = 80\%/\sqrt{E} \oplus 10\%$ (E in GeV).

In a plane orthogonal to the beam the SPD, preshower and EM are divided in three different cell-size zones (Fig. 4). The square cells have dimensions varying between about 4 cm, 6 cm and 12 cm moving from the inner to the outer region. A tower geometry has been obtained varying the cell size according to the distance from the interaction point. The smallest cell size is close to the Moliere radius so that most of the energy of an isolated shower is contained in a quartet of cells. The total number of channels in each detector is 5952.

The hadronic calorimeter is divided in two zones (Fig. 4). The cell size is about 13 cm (26 cm) in the inner (outer) region. The cell dimensions are such that each tower of HCAL matches the ECAL towers. The number of channels is 1468.

The search of the four different candidates (e, h, π^0 and γ) with highest E_T is performed in three steps

- the 2x2 cells maximum E_T deposit is searched in each ECAL and HCAL FrontEnd board (32 cells are grouped in a FE board). The selection of the highest E_T candidate at the front-end board level allows to reduce the amount of data to be transmitted, resulting in 200 candidates for the ECAL and 50 candidates for the HCAL (to be compared to the 6000 front-end channels of the ECAL and the 1500 of the HCAL). For the “local” π^0 selection, requiring two photons inside the same FE, the sum of E_T all over the FE is calculated.
- The identification of the nature of the local maxima is performed in the validation card, which groups up to 8 FE. For the validation of the electromagnetic clusters the activity in the Pre-Shower and the SPD detectors in the 2x2 cells region in front of the ECAL maxima is checked. Before performing hadronic candidates validation the E_T of the HCAL candidates is corrected for

the energy lost in ECAL. To avoid to have to connect all ECAL cells to HCAL electronics, the correction is performed looking if among the ECAL local maxima there is one lying in front of HCAL maximum. If such maximum is found the correction is performed. This approximate procedure is quite good. In fact if the correction is important, i.e. the energy released is large, it is likely revealed as a local maximum. In the validation card the “global” π^0 selection, i.e. the two photons hitting two adjacent FE, is performed adding the E_T of the candidates laying in two adjacent cards.

- The highest E_T candidate for each type is selected and sent to the L0 Decision Unit.

The L0Calo also send to L0 Decision Unit the multiplicity of deposits in the SPD and the total transverse energy measured by the HCAL.

The performance values of the L0Calo for different physics channels are shown in Table 1. To evaluate the efficiency an output rate of about 700 kHz, 100 kHz, 125 kHz, 150 kHz has been assumed respectively for hadrons, electrons, photons and neutral pions respectively. The efficiency is evaluated on events selected offline for physics studies.

The dependence of the trigger selection efficiency and reduction power as a function of the E_T threshold applied in the hadron trigger is depicted in Fig. 5.

The electronics related to the first two trigger steps is located on the calorimeter platform, where a large radiation dose is expected (less than 50 Gy during the the whole experiment lifetime), therefore the Single Event Upsets are expected to occur. As a consequence rad-hard components and triple voting technique for permanent memories are used.

4 Muon system and its use in L0

The Muon detector is composed of 5 stations interleaved with muon filter. The filter is comprised of the electromagnetic and hadronic calorimeters and three iron filters, the total interaction length corresponds to $20 \lambda_I$, therefore a muon transversing the whole system has a minimum momentum of about 8 GeV.

The multi wire proportional chamber technique (MWPC) has been adopted for all muon stations but the inner part of M1. For the inner part of M1 where the particles rate is much larger the possible alternatives are GEM or asymmetric MWPC. As described below the muon trigger is designed in such a way that information from all five muon stations is required. In order to achieve trigger efficiency of at least 95% the single station efficiency has to be higher than 99%. To ensure such a high single-station efficiency four sensitive gas gaps per station (two in M1 to reduce the material in front of the SPD and PR) are used taking the logical OR.

The lateral segmentation of the system is depicted in Fig. 6. Each station is divided in four regions with different pad granularity. Moving from an inner to an outer region the region and the pad sizes scale by a factor two. Such

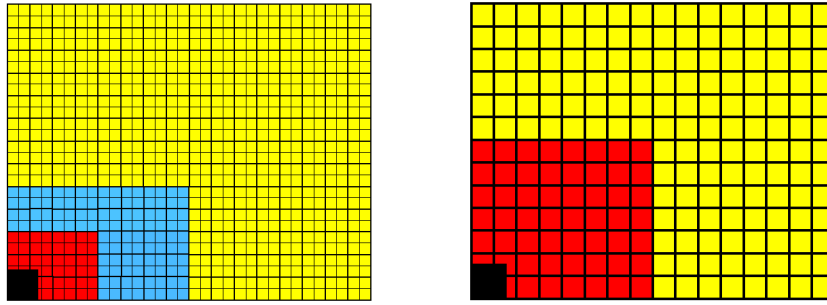


Fig. 4. The calorimeter division in zones of different cell size: on the *left* the ECAL/SPD/PR, on the *right* HCAL

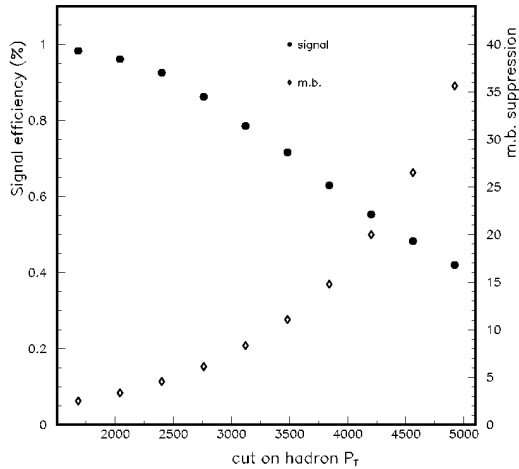


Fig. 5. The L0Calo trigger efficiency for $B \rightarrow \pi\pi$ events and the minimum bias reduction factor as a function of the E_T cut for hadrons. The trigger efficiency is evaluated on the $B \rightarrow \pi\pi$ events selected by the offline reconstruction

layout has the feature that the contribution to the P_T resolution due to the detector granularity is almost equal to the contribution due to multiple scattering over the whole X-Y surface. As a consequence the $\sigma(P_T)/P_T$ is almost constant irrespectively of where the muon track hits the station surface. The layouts in the five muon stations are projective in Y. In X the smallest pad dimension is in M2-M3, in station M1 (M4 and M5) they are a factor 2 (4) larger. The result of such segmentation is that the smallest pad is $6.3 \times 31.3 \text{ mm}^2$, while the largest is $25 \times 31 \text{ cm}^2$

The number of pads in all five stations is about 55,000. In the largest part of stations M2 to M5, where the expected particles flux is low, the pads are combined in strips reducing the number of channels to about 26,000. For further details on the Muon System see [4].

The muon trigger works as follows (Fig. 7). It combines strips in pads. Each hit pad in M3 constitutes a seed for the muon tracks search. For each seed the straight line passing through the seed and the interaction point is extrapolated to M2, M4, M5. Hit pads are looked for in these stations inside search windows, named Field Of Interest, centered on the straight-line extrapolation. If at least one hit is found inside the search window in each of the three

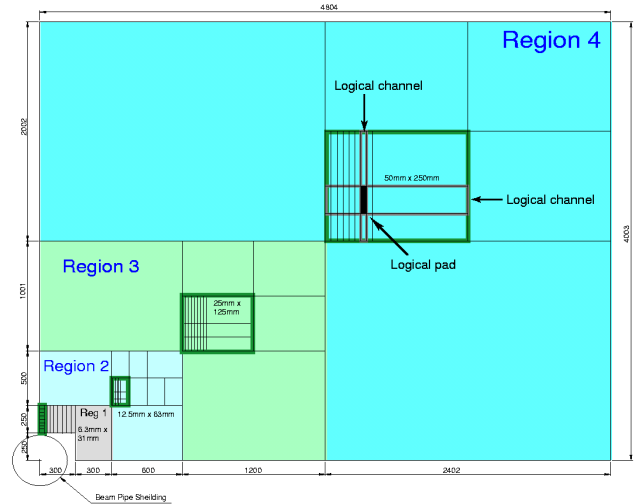


Fig. 6. Front view of a quarter of station 2, showing the dimension of the regions

stations a muon track is flagged. The seed and the closest pad in M2 are used to extrapolate to M1. When a pad is found inside the search window in M1, the P_T is calculated using the pad position in M1 and M2 and assuming the nominal interaction point as the origin of the muon track. For the calculation a look-up table is used. Up to two muon candidates per quadrant of the muon system are sent to the L0 Decision Unit.

The resolution in P_T obtained by the trigger is about 20%. The various contributions to the resolution are shown in Fig. 8.

The efficiency of the muon trigger on a sample of $B_s \rightarrow J/\psi(\mu\mu)\phi$ selected by offline reconstruction and the minimum bias suppression power as a function of the P_T cut are reported in Fig. 9.

The robustness of the L0 muon trigger has been studied increasing the hit multiplicity and worsening the detector response. The trigger shows to be robust with a relative decrease of efficiency less than 10%. Even increasing the rate of muon associated with the beam halo in the accelerator tunnel, the trigger appears to be very robust. In particular when multiplying the number of beam halo muons by a factor 10 as expected in the early days of the second year of running the efficiency decreases by 8%.

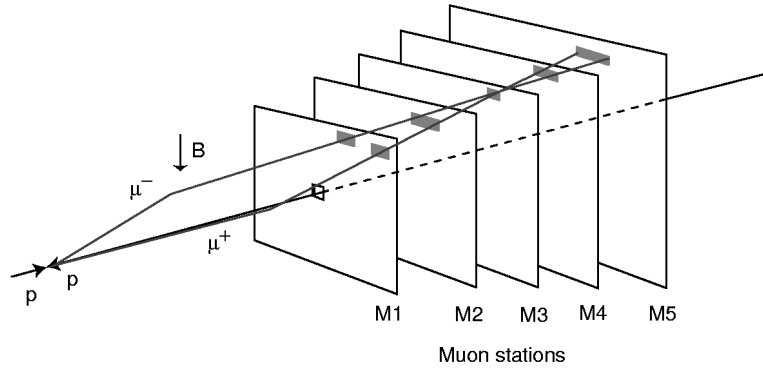


Fig. 7. Track finding by the muon trigger. Starting from the hit pad in M3, hits in M2-M5 are searched along the extrapolation through M3 and the interaction point. When hits in the three stations are found, an extrapolation on M1 using the hit in M2 and M3 is performed. If a hit is found also in M1 the P_T is measured using the direction given by hit pad positions in M1 and M2 and assuming the interaction point as the origin of the muon

Table 1. The efficiency for the different parts of the L0 calorimeter algorithm. The efficiency is evaluated on a sample of offline selected events

	inclusive efficiency (%)			
	e trig.	γ trig.	π^0 trig.	hadron trig.
$B \rightarrow \pi\pi$	5.8 ± 0.2	3.7 ± 0.2	9.9 ± 0.2	47.6 ± 0.5
$B_s \rightarrow D_s K$	5.1 ± 0.1	3.7 ± 0.1	8.2 ± 0.2	39.3 ± 0.3
$B \rightarrow J/\psi(ee)K(\pi^+\pi^-)$	32.5 ± 0.9	4.3 ± 0.4	24.5 ± 0.8	21.5 ± 0.8
$B \rightarrow K^*\gamma$	24.8 ± 1.0	38.8 ± 1.1	51.0 ± 1.1	32.7 ± 1.1

Table 2. The efficiency of the different L0 trigger subsystems. Inclusive and total efficiencies are reported for several interesting decay modes. The efficiencies are calculated on offline selected events sample

	inclusive efficiency (%)			
	μ trig.	electron trig.	hadron trigg.	all
$B \rightarrow \pi^+\pi^-$	6.8 ± 0.2	14.1 ± 0.3	47.6 ± 0.5	53.6 ± 0.4
$B_s \rightarrow D_s^-(K^+K^-\pi^-)K^+$	8.2 ± 0.2	11.6 ± 0.2	39.3 ± 0.3	46.8 ± 0.3
$B_s \rightarrow J/\psi(ee)K_S^0(\pi^+\pi^-)$	7.0 ± 0.5	37.4 ± 0.9	21.5 ± 0.8	48.3 ± 1.0
$B_s \rightarrow J/\psi(\mu\mu)\phi(K^+K^-)$	87.4 ± 0.1	8.4 ± 0.1	20.0 ± 0.2	89.7 ± 0.1
$B \rightarrow K^{*0}(K^+\pi^-)\gamma$	7.8 ± 0.6	68.1 ± 1.1	32.7 ± 1.1	72.9 ± 1.0

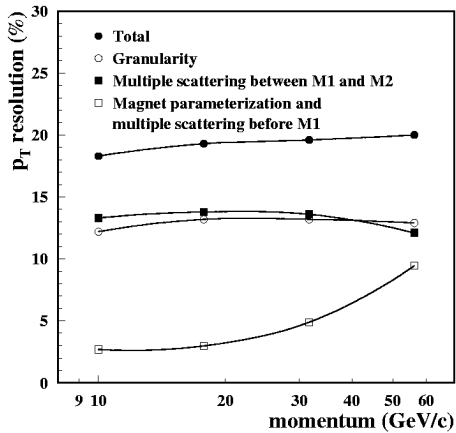


Fig. 8. The $\sigma(P_T)/P_T$ obtained by the trigger algorithm is shown as a function of the muon momentum

5 Pile-up detector and its use in L0

Two planes of silicon strip detectors are located upstream of the vertex detector, covering the pseudorapidity range $-4.2 < \eta < -2.9$. Each plane is composed of two halves of R-measuring sensors (Fig. 10), whose active area extends between 8 mm and 42 mm. The n-on-n silicon thickness is $220 \mu\text{m}$, while the pitch of the strips varies continuously along the radius between a minimum of $40 \mu\text{m}$ and a maximum of $103 \mu\text{m}$. Each strip is divided in 4 sectors of 45° each. Four neighboring strips are ORed providing 2048 binary channels toward L0. For details on the silicon detectors see [5].

The procedure adopted to identify the bunch crossing with more than one interactions is the following

- for each couple of hit channels in the same octant of the two detector planes the quantity $Z_V = (R_B Z_A - R_A Z_B)/(R_A - R_B)$ is calculated. Z_A and Z_B are the z

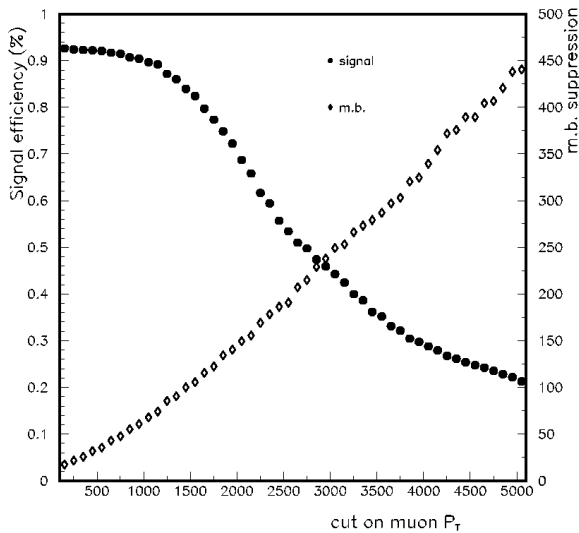


Fig. 9. The L0Muon trigger efficiency on $B_s \rightarrow J/\psi(\mu\mu)\phi$ events and the minimum bias reduction factor as a function of the P_T cut for muon. The trigger efficiency for the $B_s \rightarrow J/\psi(\mu\mu)\phi$ events is evaluated on the events selected by offline reconstruction

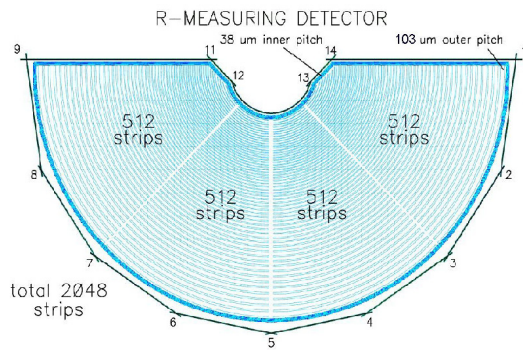


Fig. 10. One of the Pile-Up sensors

coordinate of the detector planes, while R_A and R_B are the radial positions of the hit channels. The quantity Z_V represents the Z of the origin of a tracks originating from the beamline.

- an appropriately binned histogram if filled with the Z_V values
- The highest peak in the histogram is searched for. All hits contributing to that peak are masked.
- The histogram is filled again using all the non-masked hit channels. The search for the highest peak is replicated.
- The height of the last identified peak is sent to L0 Decision Unit.

The L0PileUp will also send to L0 the multiplicity of hit channels. Such information will be useful to identify and reject “complicated” events.

The ability of the Pile-Up system to distinguish between crossings with single or multiple interactions is shown in Fig. 11. For example applying a cut on the height

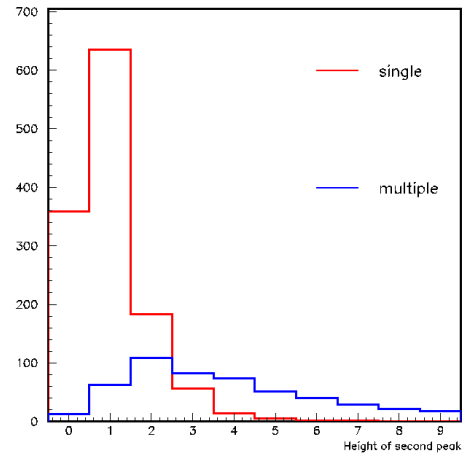


Fig. 11. Height of the second peak for single and multiple inelastic interactions is shown. The sample is composed of minimum bias events with a L0Calo or L0Muon candidate above threshold

of the second peak at 3, more than 95% of single interactions are kept while more than 60% of the multiples are rejected.

The gain in signal yield applying the Pile-Up veto depends on the decay mode and luminosity. For instance at the optimal luminosity a gain of about 10% is expected for offline reconstructed $B_s \rightarrow D_s K$ events. In the meantime the L1 trigger time decreases by more than 10%.

6 L0 decision unit and the trigger performance

The L0 Decision Unit (L0DU) receives information from Calorimeters, Muon and Pile-Up sub-triggers. Combining the data it derives one decision per crossing at 40 MHz. In particular it receives:

- 7 words from the Calorimeter sub triggers: the transverse energy of the highest E_T candidates (electron, photon, hadron, local and global π^0), the total transverse energy in HCAL, the SPD multiplicity.
- up to 8 words corresponding to the transverse momentum of the muon candidates (2 per quadrant) from the Muon sub trigger
- 2 words from the Pile-Up sub-trigger: the number of tracks outgoing the secondary vertex and the multiplicity in the system.

The L0DU has large flexibility in combining the input information to derive a decision. To obtain the performance results presented here a simple algorithm has been assumed. In particular the L0DU decision is positive if one of the calorimeters or muon candidates is above the threshold and the number of tracks from secondary vertex, the SPD multiplicity and the Pile-Up multiplicity are below threshold. A di-muon trigger is implemented: if more than one candidates is found in the muon detector the sum

of the two highest P_T candidates is calculated. In such a case the global cuts are not applied.

Using the above described algorithm the L0 trigger performance reported in Table 2 is obtained. In general the L0 efficiency is very high, even around 90% for some channels. The relative importance of the sub-triggers varies largely from channel to channel, but all sub-trigger are fundamental to select interesting events.

7 Summary

The physics goal of the LHCb experiment is the study of CP violation and rare phenomena in the b-hadrons produced in the pp collision at the LHC. The large interaction rate, about 10 MHz, must be brought down to the 200 Hz rate at which the data will be written to the permanent data storage. Such reduction will be performed by means of three trigger levels. The first level is an hardware trigger with an output rate of 1 MHz. It uses information from the calorimeters and the muon system, and selects events with high transverse energy lepton, hadron or photon

candidates. Moreover it will reject events “too complex” for following trigger levels and offline reconstruction by means of some global multiplicity cuts as multiplicity in calorimeters and in Pile-Up system or number of tracks from a second primary vertex.

The performance of the level-0 trigger are predicted to be very good, for example a full simulation has shown that an efficiency larger than 50% for $B \rightarrow \pi\pi$ and about 90% for $B_s \rightarrow J/\psi(\mu\mu)\phi$ can be reached.

References

1. Reoptimized LHCb Detector Design and Performance Technical Design Report, CERN/LHCCC,2003-030, 9 September 2003
2. T. Sjöstrand: Comp. Phys. Comm. 82(1994)74
3. LHCb Calorimeter Technical Design Report, CERN/LHCC, 2000-036
4. LHCb Muon System Technical Design Report, CERN/LHCC, 2001-010
5. LHCb VELO Technical Design Report, CERN/LHCC, 2001-011